Topographic shear and the relation of ocular dominance columns to orientation columns in primate and cat visual cortex*

Richard J. Wood† Eric L. Schwartz‡

August 26, 1998

Abstract

Shear has been known to exist for many years in the topographic structure of primary visual cortex, but has received little attention in the modeling literature. Although the topographic map of V1 is largely conformal (i.e. zero shear), several groups have observed topographic shear in the region of the V1/V2 border. Furthermore, shear has also been revealed by anisotropy of cortical magnification factor within a single ocular dominance column. In the present paper, we make a functional hypothesis: **the major axis of the topographic shear tensor provides cortical neurons with a preferred direction of orientation tuning**. We demonstrate that isotropic neuronal summation of a sheared topographic map, in the presence of additional random shear, can provide the major features of cortical functional architecture with the ocular dominance column system acting as the principal source of the shear tensor. The major principal axis of the shear tensor determines the direction and its eigenvalues the relative strength of cortical orientation preference. This hypothesis is then shown to be qualitatively consistent with a variety of experimental results on cat and monkey orientation column properties obtained from optical recording and from other anatomical and physiological techniques. In addition, we show that a recent result of (Das and Gilbert, 1997) is consistent with an infinite set of parameterized solutions for the cortical map. We exploit this freedom to choose a particular instance of the Das-Gilbert solution set which is consistent with the full range of local spatial structure in V1. These results suggest that further relationships between ocular dominance columns, orientation columns, and local topography may be revealed by experimental testing.

*We thank Gary Blasdel, Alfonso Nieto-Castanon, and Michael Cohen for helpful discussion and useful suggestions in improving this work.

†rjwood@cns.bu.edu

‡eric@thing4.bu.edu

1 The local spatial structure of V-1

For many years, shear has been known to exist in the topographic structure of primary visual cortex, but has received little attention in the modeling literature. This note is concerned with the anisotropy of the retino-cortical mapping (i.e. shear) and the role this anisotropy plays in cortical function. The global topographic map structure of V-1 is roughly approximated by a complex logarithmic map of retinal coordinates (Schwartz, 1977) and is more accurately modeled in terms of a numerical conformal mapping that is constrained by the shape of the boundaries of V-1 (Schwartz, 1994). The main disagreement of this model with experiment is provided by the existence of topographic distortions near the representation of the V1-V2 border (van Essen et al., 1984; Schwartz, 1994). In addition to this large scale shear, (LeVay et al., 1975) and (Blasdel et al., 1995) have reported that the ocular dominance column system locally distorts the cortical tissue by 60-100%. It appears that this local shear adds randomly, since the global topographic structure of V1 is generally consistent with the conformal hypothesis (Schwartz, 1993).

The key hypothesis of the present paper is that afferent summation by isotropic cortical dendritic fields of an underlying sheared topography provides a well defined orientation axis for cortical cells. We show that this hypothesis is sufficient to qualitatively account for a wide variety of experimental measurements in cortical spatial structure[1].

The V1 orientation column pattern, as measured by optical recording (Blasdel and Salama, 1986), can be qualitatively accounted for by band-pass filtering of random spatial vector fields (Rojer and Schwartz, 1990), and also by **low-pass** filtering (Schwartz and Rojer, 1991; Schwartz and Rojer, 1992; Schwartz and Rojer, 1994). The latter result, which is novel with respect to previous models, is due to the fact that the so-called "pin-wheel" or "vortex" orientation pattern in visual cortex is really a form of topological singularity ("topological noise") and is thus generic and not dependent on any modeling details other than the introduction of a local correlation of orientation at nearby spatial positions (Schwartz and Rojer, 1991; Tal and Schwartz, 1997). The model presented in this paper qualitatively accounts for, and is motivated by, the following seven experimental findings:

Experimental result 1 (Ocular dominance column induced topographic shear) *Local cortical magnification is anisotropic, and the anisotropy is aligned with the local ocular dominance column structure (Blasdel et al., 1995; LeVay et al., 1975)*

Experimental result 2 (Vortex centration) *In both the cat (Hubener et al., 1997) and the monkey (Blasdel et al., 1995), the centers of V-1 vortex centers are peaked around the center of the ocular dominance column.*

Experimental result 3 (Orthogonality) *In both the cat (Hubener et al., 1997) and the monkey (Blasdel et al., 1995), the iso-angle orientation contours (i.e. the boundaries of orientation columns) tend to intersect the ocular dominance column boundaries at right angles.*

Experimental result 4 (Graded orientation tuning) *Receptive fields of cortical neurons near the borders of the ocular dominance columns are more "tuned" (i.e. are less isotropic) than one nears the singularities, or centers (Livingstone and Hubel, 1988).*

Experimental result 5 (Graded Spatial Frequency tuning) *Receptive field size is largest in the center, and falls off towards the boundaries of the OD columns (Hubener et al., 1997)*

Experimental result 6 (Existence of local map structure) *(Das and Gilbert, 1997) have shown that there is a detailed local topographic map in cat V-1 and that there is an approximately linear relationship between the magnitude of receptive field movement and the magnitude of orientation gradient at each point in the cortex* [2]

[1] We don't concern ourselves here with the details of lateral inhibition and/or excitation, which are presumed to account for the **enhancement** of orientation tuning.

[2] This is a surprising and important result in view of the standard understanding, originating with (Hubel and Wiesel, 1974), that local "scatter" of receptive field structure is comparable to the size of cortical hypercolumns. (Das and Gilbert, 1997) showed that this was likely due to residual eye motion in the paralyzed preparation and that when the eye was fixed to a ring the "scatter" was negligible! The results of Das and Gilbert suggest that there is a detailed local map structure in V-1, on the scale of a cortical hypercolumn, whose properties are intimately related to the spatial layout of orientation tuning.

Experimental result 7 (Monocular core zones in primate ocular dominance columns) *(Horton and Hocking, 1998) have shown that in layer IVc of primate striate cortex there is a periodic segregation of afferent input into central "core zones" which come from one eye, and "binocular border strips" in which both eyes contribute input. Our interpretation of these results is that since cortical cell density is constant, the "squeeze" necessary to accommodate alternating monocular and binocular zones within a single ODC would be expected to cause a periodic, or oscillating variation in the local topographic map structure.*

2 Topographic shear waves

We adopt coordinates (x, y) for the cortex, and coordinates (u, v) for the visual field (or retina). $(u(x, y), v(x, y))$ maps points in the cortex to corresponding points in the visual field and is the inverse of the usually defined topographic map function (Schwartz, 1994)). In this paper, we refer to two models. The first model is a simple analytic version of the system that we analyze, and the second is a more realistic, spatial noise-based model. For the simple analytic model, we take x perpendicular to the long axis of the ocular dominance columns and y parallel to the long axis. We model the $ODC(x, y)$ function[3] in this case with a simple sinusoidal variation perpendicular to the y-axis. In the noise based model, we construct the function $ODC(x, y)$ via filtering spatial white noise as in earlier work (Rojer and Schwartz, 1990). The familiar "zebra-skin" pattern of ODC is produced by thresholding $ODC(x, y)$. We emphasize that $ODC(x, y)$ is a continuous (more accurately random) function, whose cross-section resembles a noisy sinusoid (or **is** a sinusoid in the simple analytic model). Our hypothesis is that **we assume that cortical topography is deformed in a manner proportional to the function** $ODC(x, y)$:

$$u(x, y) \;=\; x + ODC(x, y); \qquad\qquad v(x, y) \;=\; y \tag{1}$$

This method of representing a local deformation is commonly used in fluid mechanics, where the sinusoidal components are interpreted as the principal modes of the deformation. This deformation is called an "oscillating shear wave". In the present context, the main justification for using this form of map function is that it provides the needed link between the ODC structure itself, cortical topography, and the orientation column system. Our assumption states that the shear is non-constant on the scale of a single hypercolumn and is minimal in the center of the ODC and rises monotonically towards the ODC boundaries.

3 Simple analytic model

The results of this paper now follow from an analysis of the structure of the dilation and pure shear components of the Jacobian matrix of the topographic shear wave.

Cortical maps and the Jacobian. The differential structure of a regular 2D mapping is represented as the sum of a pure dilation D, a rotation A, and a pure shear T. For a regular map $F : R^2 \to R^2$; $F : (x, y) \mapsto (u(x, y), v(x, y))$, the Jacobian matrix, which represents dF, is $\mathbf{J} = \begin{bmatrix} u_x & u_y \\ v_x & v_y \end{bmatrix}$. As mentioned in earlier work in the anatomical context (Schwartz, 1984), and as is standard in continuum mechanics (Segal, 1977), we express the Jacobian in terms of a pure dilation $\mathbf{D}$ (diagonal matrix), a rotation $\mathbf{A}$ (anti-symmetric matrix) and a pure shear $\mathbf{T}$ (traceless matrix):

$$\mathbf{J} = \begin{bmatrix} 1/2(u_x + v_y) & 0 \\ 0 & 1/2(u_x + v_y) \end{bmatrix} + \begin{bmatrix} 0 & 1/2(u_y - v_x) \\ 1/2(v_x - u_y) & 0 \end{bmatrix} + \begin{bmatrix} 1/2(u_x - v_y) & 1/2(u_y + v_x) \\ 1/2(u_y + v_x) & -1/2(u_x - v_y) \end{bmatrix} \tag{2}$$

As noted, the shear $\mathbf{T}$ is a traceless symmetric tensor field: $\mathbf{T} = \begin{bmatrix} a(x, y) & b(x, y) \\ b(x, y) & -a(x, y) \end{bmatrix}$

[3] Following (Rojer and Schwartz, 1990), we term the result of filtering spatial 2D random data with a band-pass filter the ODC function.

Eigenvalue of the shear tensor. The eigenvalue λ of the shear tensor represents an elongation by an amount λ along the major principal axis and a decrease by λ along the minor principal axis. For the simple analytic model: $ODC(x,y) = sin(\frac{\pi x}{W}), a = \frac{1}{2}(u_x - v_y) = ODC(x,y)_x = \frac{\pi}{2W}cos(\frac{\pi x}{W})$ and $b = \frac{1}{2}(u_y + v_x) = ODC(x,y)_y = 0$, and $\lambda = \sqrt{a^2+b^2} = |\frac{\pi}{2W}cos(\frac{\pi x}{W})|$. We identify λ with the "strength" of orientation tuning at the cortical location (x,y), since it represents the amount of "stretching" of an infinitesimal cortical circle to a retinal ellipse. λ is minimal at the vortex center, and increases monotonically towards the ODC boundaries which is in agreement with observation of strength of orientation tuning.

Eigenvectors of the shear tensor. By our assumption, the orientation function, $\theta(x,y)$, represents the major axis of the shear tensor and is the direction of orientation tuning [4,5]. Thus, in the center of the ODC, where λ is minimal, there is minimal orientation tuning (i.e. circular receptive fields). Near the ODC boundaries, shear is maximal and orientation is, in the absence of noise, exclusively perpendicular to the local ODC boundary. **At this point, the model is not biologically correct, since it provides only a single orientation tuning direction, which is horizontal.** However, when orientation noise (i.e. noise in the local shear function) is added and spatially filtered, the more familiar orientation vortex is produced. Thus, the full range of orientation tuning is provided entirely by noise in the shear tensor, while the dominant spatial trends are determined by the underlying oscillating shear term.

The role of vorticity. It is convenient for visualization to define a vector field whose integral curves run in the same direction as the minor principle axis of the shear tensor. This is the same direction as the gradient of the orientation function $\theta(x,y)$. We choose this vector field to be: $\vec{s}(x,y) = (-b(x,y), a(x,y))$.

Since $\vec{s}$ is parallel to $\nabla\theta(x,y)$, the center of a "vortex" will correspond to a peak in the magnitude of the vorticity $\omega = -\frac{1}{2}\nabla \times \vec{s}$ of $\vec{s}$ and this peak vorticity should (statistically) correspond to the center of the ODC [6].

$$\vec{\omega}(0,0,z) = -\frac{1}{2}\nabla \times \vec{s}(x,y,0) = (0,0,-\frac{1}{2}(-b(x,y,0)_y + a(x,y,0)_x)) \quad (3)$$

$$\vec{\omega}(0,0,z) = \frac{\pi^2}{4W^2}(0,0,sin(\frac{\pi x}{W})) \quad (4)$$

The maximum level lines of the magnitude of vorticity lie along x=W/2 which represents the centers of the OD columns. The peaking of the vorticity in the center of OD columns provides the "centration" of cortical vortices.

Thus, when random orientation noise is added to the model in the form of random shear, random vorticity is added as well but the underlying distribution of vorticity, which is peaked in the center of the ODC, will still favor vortex formation in the centers of the OD columns. Figure 1 clearly shows this behavior in the spatial noise model.

In order to account for the remaining experimental results mentioned at the beginning of this paper, we will consider a recent important experimental result of (Das and Gilbert, 1997).

[4]Both the minor and major axes of the shear tensor are described by $\tan 2\theta = b/a$ because the axes are orthogonal and $\tan 2\theta$ is invariant to $\theta \rightarrow \theta + \pi/2$. The correct choice of the direction of the major principle axis is found by solving the characteristic equation of the shear tensor and is given by $\tan(\theta(x,y)) = b/(a+\lambda)$.

[5]The shear of the inverse topographic map describes retinal ellipses corresponding to cortical circles. The shear of the topographic map describes cortical ellipses corresponding to retinal circles. The direction of the principal shear axis of the inverse topographic map runs horizontally in the retina (the "u" axis in the present example). The direction of the principle axis of the shear tensor of the topographic map runs parallel to the y-axis in the cortex (parallel to the local ODC boundary in the noise based model).

[6]Alternatively, we could have defined our shear vector field to be orthogonal to $\vec{s}$, i.e. $\vec{s'} = (a(x,y), b(x,y))$. The integral curves of $\vec{s'}(x,y)$ are in the direction of the iso-angle lines. With this choice, we would locate the vortex centers by the divergence of s'.

4 The Das-Gilbert Ratio

(Das and Gilbert, 1997) reported a linear relationship between receptive field shift, measured in the visual field, and orientation change corresponding to small spatial steps in the cortex . The Das-Gilbert criterion is mathematically stated as follows: [7]

$$\left\| \begin{bmatrix} u_x & u_y \\ v_x & v_y \end{bmatrix} \begin{bmatrix} dx \\ dy \end{bmatrix} \right\| = K \left\| \nabla\theta(x,y) \begin{bmatrix} dx \\ dy \end{bmatrix} \right\| \tag{5}$$

Equation 5 states the relationship between the change in visual field position of the underlying cortical map (left hand side) to the change in orientation corresponding to a small cortical step $(dx, dy)'$. By equating the terms of the quadratic form thus obtained, we then study the following algebraic system:

$$u_x^2 + v_x^2 = K^2\theta_x^2 \qquad u_y^2 + v_y^2 = K^2\theta_y^2 \qquad u_x u_y + v_x v_y = K^2\theta_x\theta_y. \tag{6}$$

A solution to these equations is provided by the following geometric reasoning: They describe the norm of a vector $(u_x, v_x)^T$ equal to $K^2\theta_x^2$, the norm of a vector $(u_y, v_y)^T$ equal to $K^2\theta_y^2$, and the inner product of $(u_x, v_x)^T$ and $(u_y, v_y)^T$ equal to $K^2\theta_x\theta_y$ which requires that the two vectors be parallel or anti-parallel. The direction, which we will parameterize as α, of the line along which the two vectors are parallel or anti-parallel is not specified. This corresponds to the under-determined nature of of equation 5 since there are four unknowns, the components of the Jacobian, and only three equations. Thus, the Jacobian of a map which satisfies equation 5 is in terms of the parameter α: [8]

$$\mathbf{J_{DG}}(\alpha) = K \begin{bmatrix} \theta_x \cos\alpha & \theta_y \cos\alpha \\ -\theta_x \sin\alpha & -\theta_y \sin\alpha \end{bmatrix} = \mathbf{D_{DG}}(\alpha) + \mathbf{A_{DG}}(\alpha) + \mathbf{T_{DG}}(\alpha) \tag{7}$$

Equation 7 indicates that there are an infinite family of solutions, parameterized by the angle α, which all satisfy the Das-Gilbert criterion of equation 5. Therefore, we choose the value of α which causes the shear vector component of the Das-Gilbert solution to be proportional to our previous shear tensor, which will now be called $\mathbf{T_0}$, with components a_0 and b_0. We do this by solving the following equations for α:

$$a_0 = K' a_{DG} = K'(\theta_x \cos(\alpha) + \theta_y \sin(\alpha)) \qquad b_0 = K' b_{DG} = K'(\theta_y \cos(\alpha) - \theta_x \sin(\alpha)) \tag{8}$$

where we use the notation a_{DG} and b_{DG} to represent the components of the shear tensor of the Jacobian $\mathbf{J_{DG}}$. By rewriting the equation above as:

$$\begin{pmatrix} a_0 \\ b_0 \end{pmatrix} = K' \begin{bmatrix} \cos\alpha & \sin\alpha \\ -\sin\alpha & \cos\alpha \end{bmatrix} \begin{pmatrix} \theta_x \\ \theta_y \end{pmatrix} \tag{9}$$

it can be seen that α represents the rotation necessary to point $\nabla\theta(x,y)$ in the same direction as $(a_0, b_0)^T$ and it immediately follows that $K' = \sqrt{{a_0}^2 + {b_0}^2}/\|\nabla\theta\| = \lambda/\|\nabla\theta\|$. Note that since the quantity b_0/a_0 determines the direction of the principal axes of the shear tensor and $b_0/a_0 = b_{DG}/a_{DG}$ by construction, the original oscillating shear tensor and the Das-Gilbert solution have shear tensors whose principle axes are parallel. This is the main point of this section of the paper: to retain the original structure of the pure shear component of the oscillating shear wave, but to substitute the dilation and rotation components of a Das-Gilbert solution. The result is the final Jacobian we assume for the cortical inverse map function:

$$\mathbf{J}_{cortex} = \mathbf{D}_{DG}(\alpha) + \mathbf{A}_{DG}(\alpha) + \mathbf{T}_0 \tag{10}$$

[7] In the following, we ignore the small constant term in the linear regression reported by Das and Gilbert, so that orientation gradient is taken to be proportional to receptive field shift.

[8] Note also that these solutions are singular: the determinant of the Jacobian matrix is zero. The singularity could be removed by adding in a constant in the linear regression, which we have discarded to simplify the analysis. This is not a problem, however, since we add these singular Jacobian terms to a generally non-singular (e.g. random) map in the final stages of the algorithm, presented below, and the constant re-emerges in the final regression as shown in Figure 1.

Note that $\mathbf{J}_{cortex}$ is not a solution to the Das-Gilbert equation, which would require that the third component to be $\mathbf{T}_0/K' = \mathbf{T}_{DG}$. Thus, our result for J_{cortex} describes a map whose dilation and rotation components are particular solutions to the general Das-Gilbert constraint of equation 6, but whose pure shear component is identical to that produced by the oscillating shear wave assumption of Equation 1.

5 Full simulation

We now state, in detail, our algorithm: Step 1. Generate random scalar noise to produce ODC(x,y) as in earlier work (Rojer and Schwartz, 1990; Schwartz and Rojer, 1994). Step 2. Construct a local map function, using ODC(x,y), of the form stated in equation 1. Step 3. Add noise to the Jacobian of the map function and apply a band pass filter to produce orientation singularities as in (Rojer and Schwartz, 1990; Schwartz and Rojer, 1994). Step 4. Extract the $\mathbf{D}_0, \mathbf{A}_0$, and $\mathbf{T}_0$ components of the Jacobian matrix of this map function, as outlined above. Construct the shear-vector field associated with the direction $\tan 2\phi = b/a$ and eigenvalue $\lambda = \sqrt{a^2 + b^2}$ of pure shear component of the Jacobian matrix of the map function. Step 4. Construct the three Das-Gilbert Jacobian matrixes by choosing α as a solution of equation 8 such that the Das-Gilbert shear tensor, $\mathbf{T}_{DG}$, is proportional to the original shear-tensor field $\mathbf{T}_0$. Step 5. Construct a new Jacobian using the Das-Gilbert Jacobian and the original Jacobian as follows: $\mathbf{J}_{cortex} = \mathbf{D}_{DG}(\alpha) + \mathbf{A}_{DG}(\alpha) + \mathbf{T}_0$.

The results of performing steps 1-5 above, on a realistic random noise field, are shown in Figures 1 and 2. Figure 1 shows that our model has vortices centered in the ODC, the proper behavior of iso-angle lines tending to intersect ODC boundaries at right angles, and a qualitative fit to the Das-Gilbert result. Figure 2 demonstrates graded spatial frequency tuning and graded orientation tuning as well as the generation of realistic orientation singularities. As our simple analytic model indicates, our simulation is in qualitative agreement with all seven experimental constraints presented above.

6 Summary

In summary, we have demonstrated an oscillating shear wave solution for cortical topography which is qualitatively consistent with a wide range of experimental observations. In particular, we have shown how the ocular dominance column system can influence an otherwise random, or noisy topographic shear such that the associated vorticity is maximal in the center of the ODC. This provides "centration" of vortex structure. The same mechanism causes the eigenvalue of the shear tensor to be minimal in the center of the ODC, thus providing graded orientation tuning which is minimal in the center and maximal at the boundaries of the ODC. The band-pass filter we used to produce the vortex pattern is oriented orthogonally to the ODC boundaries, which produces, and controls, the extent of "orthogonality". Finally, the Das-Gilbert property is explicitly forced by manipulating the dilation and rotation components of the Jacobian to have the Das-Gilbert form, while retaining the shear component of the oscillating shear solution. This also has the effect of causing the "graded spatial frequency" property. Finally, the Horton-Hocking observation of monocular core zones and binocular flanking structure within a single ODC is key in providing some reason to believe that the local cortical topography may indeed have an oscillating shear structure!

Our experience to date with these simulations suggests that there is a fair degree of independence of all of these properties. We have observed that it is possible to separately control, within limits, the relative strength of the various effects. This is promising for more quantitative fitting of the available data, since in this short preliminary letter, we have not provided actual statistical fits to the current experimental data.

In a forthcoming paper, we plan to investigate in more detail the range over which it is possible to locally integrate the Jacobian that we have constructed, and also the effects of varying the parameters of this model.

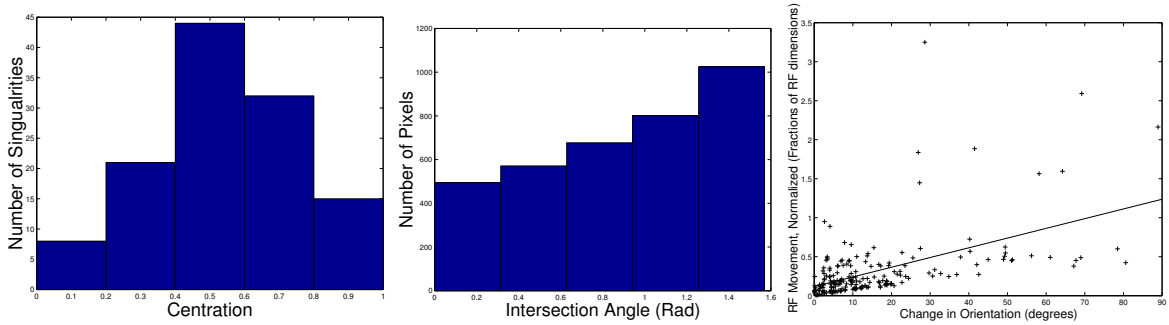

Figure 1: Left: Centration histogram. Center: Orthogonality histogram. Right: Das-Gilbert plot.

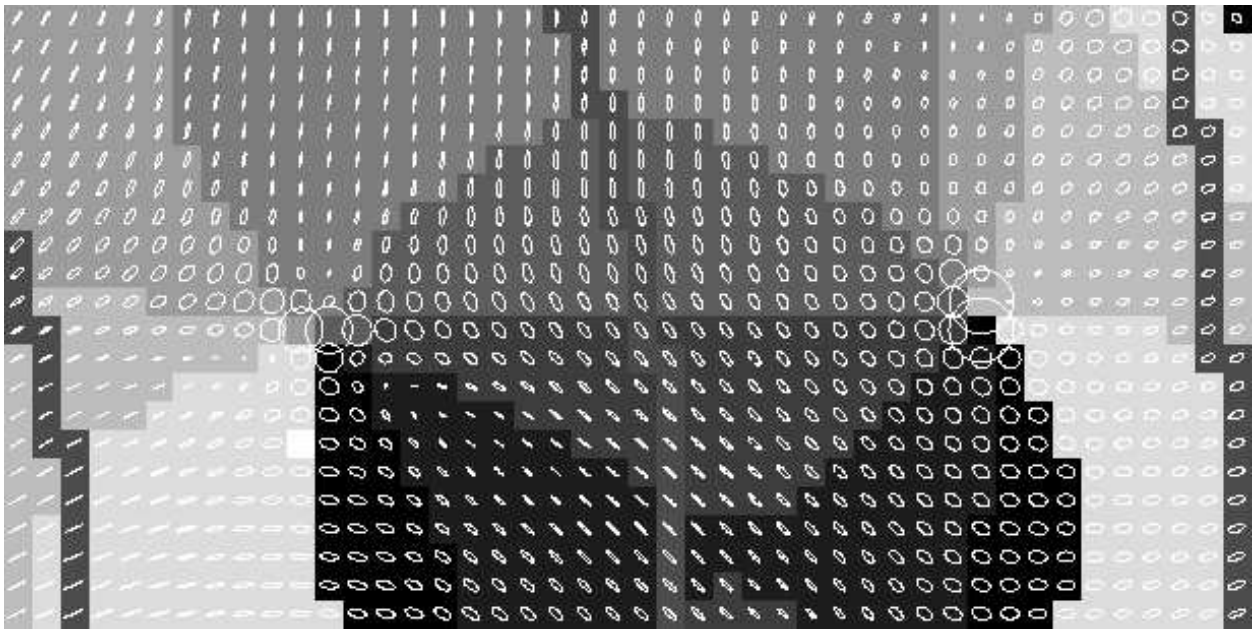

Figure 2: A sample of a vortex-ODC plot for the random noise simulation. Overlaid are small circles to which the dilation and shear components of J_{cortex} have been applied. Note that near the singularity centers, the circles are large with little anisotropy. In most directions, the circles become smaller and increase in anisotropy away from the singularity centers. Gray scale represents orientation tuning. Dark gray bands that appear to the left, middle, and right are ODC borders.

References

Blasdel, G., Obermeyer, K., and Kiorpes, L. (1995). Organization of ocular dominance and orientation columns in the striate cortex of neonatal macaque monkeys. *Visual Neurosciences*, 12:12.

Blasdel, G. and Salama, G. (1986). Voltage sensitive dyes reveal a modular organisation in monkey striate cortex. *Nature*, 321:579–585.

Das, A. and Gilbert, C. D. (1997). Distortions of visuotopic map match orientation singularities in primary visual cortex. *Nature*, 387(6633):594–598.

Horton, J. C. and Hocking, D. R. (1998). Monocular core zones and binocular strips in primate striate cortex revealed by the contrasting effects of enucleation, eyelid suture and retinal laser lesions on cytochrome oxidase activity. *J. Neuroscience*, 18:5433–5455.

Hubel, D. H. and Wiesel, T. N. (1974). Sequence regularity and geometry of orientation columns in the monkey striate cortex. *J. Comp. Neurol.*, 158:267–293.

Hubener, M., Shoham, D., Grinvald, A., and Bonhoeffer, T. (1997). Spatial relationships among three columnar systems in cat area 17. *Journal of Neuroscience*, 17:9270–9284.

LeVay, S., Hubel, D. H., and Wiesel, T. N. (1975). The pattern of ocular dominance columns in macaque visual cortex revealed by a reduced silver stain. *Journal of Comparative Neurology*, 159:559–576.

Livingstone, M. and Hubel, D. (1988). Segregation of form, color, movement and depth: Anatomy, physiology, and perception. *Science*, 240:740.

Rojer, A. and Schwartz, E. L. (1990). Cat and monkey cortical columnar patterns modeled by bandpass-filtered 2D white noise. *Biological Cybernetics*, 62:381–391.

Schwartz, E. and Rojer, A. (1994). Cortical hypercolumns and the topology of random orientation maps. In *ICPR Proceedings*, ICPR-12. International Conference on Pattern Recognition.

Schwartz, E. L. (1977). Spatial mapping in primate sensory projection: analytic structure and relevance to perception. *Biological Cybernetics*, 25:181–194.

Schwartz, E. L. (1984). Anatomical and physiological correlates of human visual perception. *IEEE Transactions on Systems, Man and Cybernetics*, SMC-14:257–271.

Schwartz, E. L. (1993). Topographic mapping in primate visual cortex: Anatomical and computational approaches. In Kelly, D. H., editor, *Visual Science and Engineering: Models and Applications*. Marcel Dekker.

Schwartz, E. L. (1994). Computational studies of the spatial architecture of primate visual cortex:columns, maps, and protomaps. In Peters, A. and Rocklund, K., editors, *Primary Visual Cortex in Primates*, volume 10 of *Cerebral Cortex*. Plenum Press.

Schwartz, E. L. and Rojer, A. S. (1991). Cortical hypercolumns and the topology of random orientation maps. Technical Report 593, Courant Institute of Mathematical Sciences, 251 Mercer Street.

Schwartz, E. L. and Rojer, A. S. (1992). A computational study of cortical hypercolumns and the topology of random orientation maps. *Society for Neuroscience Abstracts*, 18:742.

Segal, L. A. (1977). *Mathematics Applied to Continuum Mechanics*. MacMillan, New York, NY.

Tal, D. and Schwartz, E. (1997). Topological singularities in cortical orientation maps: the sign principle correctly predicts hypercolumn structure in primate visual cortex. *Network*, 8:229–238.

van Essen, D. C., Newsome, W. T., and Maunsell, J. H. R. (1984). The visual representation in striate cortex of the macaque monkey: Asymmetries, anisotropies, and individual variability. *Vision Research*, 24:429–448.